Constraint of symmetry energy slope using neutron skins of ^{48}Ca, ^{64}Ni, ^{124}Sn, and ^{208}Pb and its impact on neutron star radius*

Y. Huang (黄宇)[1,2] K. X. Huang (黄开轩)[3] Z. X. Yang (杨祖星)[4] X. L. Tu (涂小林)[2†]
J. N. Hu (胡金牛)[3] J. T. Zhang (张景涛)[2] J. F. Han (韩纪锋)[1]

[1]Key Laboratory of Radiation Physics and Technology of the Ministry of Education, Institute of Nuclear Science and Technology, Sichuan University, Chengdu 610064, China
[2]Institute of Modern Physics, Chinese Academy of Sciences, Lanzhou 730000, China
[3]School of Physics, Nankai University, Tianjin 300071, China
[4]RIKEN Nishina Center, Wako, Saitama 351-0198, Japan

Abstract: We constrain the symmetry energy slope L at the saturation density using the neutron skin values of ^{48}Ca, ^{64}Ni, ^{124}Sn, and ^{208}Pb determined by various experiments. The resulting L of 50(6) MeV is consistent with the world-averaged value from different observables and methodologies. Furthermore, the implications of newly constrained L on the radius determinations of 1.4 solar-mass neutron stars are also discussed based on the established $R_{1.4}$-L linear relationships by the DD-ME2 and TW99 EoS families.

Keywords: neutron skin, symmetry energy slope, neutron star radius

DOI: **CSTR:**

I. INTRODUCTION

The equation of state (EoS) of isospin asymmetric nuclear matter plays an important role in researches of nuclear reaction, structure, and astrophysics [1]. For example, bulk properties of neutron stars are mainly governed by the EoS [1−4]. Many investigations indicate that there are significant correlations between neutron star radii and the EoS parameters, namely, the symmetry energy slope L at the saturation density ρ_0, the nuclear matter incompressibility coefficient K_0, and the skewness parameter Q_0 [4−9]. Especially, the radii of neutron stars with density $\rho \sim \rho_0$ are primarily determined by the slope L [4]. Owing to the importance including but not limited to that mentioned above, many attempts are made to precisely determine the EoS parameters [7, 10]. The K_0 was constrained with a precision of about 10 percents to be 240(20) MeV by giant resonance [11, 12], which agrees with the recent results [13]. However, the deduced L values at ρ_0 by different methodologies have a large spread from about 30 to 110 MeV, more details see review article [14]. In particular, due to lack of sensitive observables, the Q_0 is still poorly known. Theoretical values for the Q_0 are in the range of ~ −1000 to ~ 1000 MeV [15].

Similar to the neutron star radii, it is well known that neutron skins formed in heavy nuclei with an excess of neutron over proton are also sensitive to the slope L at ρ_0 [16]. Since the linear relationships were established based on different effective nucleon-nucleon interactions of the self-consistent mean-field models [16], neutron skin thicknesses ΔR_{np} as the difference of neutron and proton distribution rms radii in nuclei, namely $\Delta R_{np} = R_n - R_p$, have been widely employed to constrain the slope L. Theoretical progresses also promote the developments of novel experimental methods for neutron distribution radius measurements [17−26]. Recently, the model-dependent ΔR_{np} data for the stable Ca, Ni, Sn, and Pb isotopes were compiled, and the evaluated ΔR_{np} values have a high precision of around 0.02 fm [27]. These compiled ΔR_{np} data [27] are taken from different experiments related to hadron scatterings [18, 24, 28], interaction cross sections [25, 29], giant resonances [30, 31], and antiprotonic atoms [22, 32]. Based on the compiled ΔR_{np} data, separate trends of ΔR_{np} versus relative neutron excess, $\delta = (N-Z)/A$, were observed for the Ca, Ni, Sn, and Pb isotopic chains [27], where N, Z, and A are neutron, proton, and mass numbers, respectively. In addition, the parity-violating electron scattering also provides a so-called mode-independent approach to determine ΔR_{np} in nuclei [23, 33]. With this method, the ΔR_{np} of ^{48}Ca and ^{208}Pb were determined by the CREX and PREX collaboration groups [23, 33], respectively. Although the tension of the

Received 5 March 2025; Accepted 16 May 2025

* This work is supported in part by the National Key R&D Program of China (Grant No. 2023YFA1606401) and by the NSFC (Grants No. 12375115 and No. 12121005)

† E-mail: tuxiaolin@impcas.ac.cn

CREX-PREX neutron skins with other experimental and theoretical results was widely discussed from the perspective of physics [34−37], the possibility of statistical fluctuations was also mentioned by Refs. [38−40]

The ΔR_{np} data from different experimental methods would be helpful to reduce the model-dependent effects of single experimental data [41]. For instance, using the ΔR_{np} of Sn isotopes from different experiments, highly precise L values at different densities have already been obtained in Refs. [42, 43]. We note that, the compiled neutron skin data from different experimental methods reproduce the predicted ΔR_{np} separate structure of Ca, Ni, Sn, and Pb isotope chains by the SLy4 interaction [27]. This would indicate that these compiled neutron skin data are reliable. Therefore, it is interesting to precisely constrain the symmetry energy slopes L at the saturation density using the compiled ΔR_{np} data [27], and to address their impacts on the neutron star radii at 1.4 solar-mass ($1.4\,M_{\odot}$).

II. DETERMINATION OF SYMMETRY ENERGY SLOPE

As known, the symmetry energy slope L at the saturation density can be sensitively constrained by the ΔR_{np} of heavy nuclei with large neutron-to-proton values [43, 44]. Therefore, for each isotope chain tabulated in Ref. [27], we only adopt the ΔR_{np} data of magic nucleus with the maximum neutron-to-proton value, namely ^{48}Ca, ^{64}Ni, ^{124}Sn, and ^{208}Pb, to determine the slope L. It would also be helpful to reduce the effects of possible ΔR_{np} isotope-dependent deviation on the L extraction through balancing the contribution of each isotope chain. To constrain the L in this work, the ΔR_{np} are analyzed via the chi-square χ^2_j defined here as

$$\chi^2_j = \sum_{k=1,i=1}^{M,N} \frac{[\Delta R^{\rm exp}_{\rm np}(k,i) - \Delta R^{\rm th}_{\rm np}(k,j)]^2}{[\delta \Delta R^{\rm exp}_{\rm np}(k,i)]^2}, \qquad (1)$$

where $k = 1,2.....M$, stands for ^{48}Ca, ^{64}Ni, ^{124}Sn, and ^{208}Pb, respectively. $i = 1,2.....N$, with N the number of adopted neutron skin thicknesses for nucleus k. $\Delta R^{\rm th}_{\rm np}(k,j)$ ($j = 1,2.....28$) is the theoretical neutron skin thickness of nucleus k corresponding to the effective interaction j. The randomly adopted effective interactions are Z, Es, E, Zs, Zs* [45], SIII [46], SkP [47], SkS1 [48], SkT6, SkT7 [49], RATP [50], SGII [51], SkS2 [48], SkM* [52], SLy4 [53], SkM [54], DD-ME2 [55], SkS3 [48], TW99 [56], PKO2, PKO3 [57], PKDD [58], PKO1 [59], PK1 [58], NL3 [60], NL-Z2 [61], NL-Z [62], and NL1 [63]. They are labeled with numbers from 1 to 28, respectively, as shown in Fig. 1. Each effective interaction corresponds to a specific L value. These interactions cover a large L range from about −50 to 140 MeV. $\Delta R^{\rm exp}_{\rm np}(k,i)$ and $\delta \Delta R^{\rm exp}_{\rm np}(k,i)$ are the ith experimental neutron skin thickness and error for nucleus k, respectively.

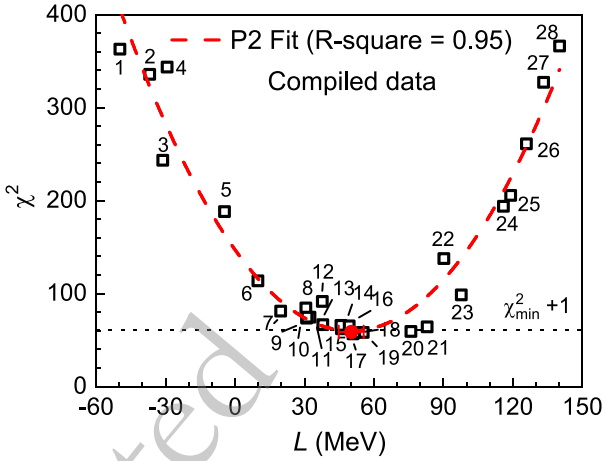

Fig. 1. (color online) The slope L versus χ^2 obtained by the compiled forty-nine model-dependent ΔR_{np} of ^{48}Ca, ^{64}Ni, ^{124}Sn, and ^{208}Pb, see Table I in Ref. [27] for details on the ΔR_{np} data. The dashed line denotes the quadratic polynomial (P2) fit with a R-Square value of 0.95. The filled red circle with error bar represents the extracted L result at the minimum χ^2. The used interaction parameter sets are labeled with numbers from 1 to 28, see text for details.

First of all, the compiled 49 model-dependent ΔR_{np} of ^{48}Ca, ^{64}Ni, ^{124}Sn, and ^{208}Pb [27] are adopted to constrain the L. These data are available in Table I in Ref. [27], which are obtained by various experiments, see Ref. [27] and references cited therein for details. The obtained χ^2 as a function of L is plotted in Fig. 1. In the χ^2 calculations, see Eq. (1), only the reported experimental errors of neutron skins are considered. The scattering of the χ^2 data points would be mainly caused by the difference of interaction models. Subsequently, the obtained χ^2 as a function of L is fitted by the quadratic polynomial (P2) function, namely, $\chi^2 = aL^2 + bL + c$. Then, a L of 50(6) MeV is deduced at the minimum χ^2, $\chi^2_{\rm min}$, via the P2 fit function. The final error of L includes the uncertainties from fitting parameters and statistics. The L uncertainty caused by fitting parameters is mainly originated from the model difference. As shown in Fig. 1, the obtained $\chi^2_{\rm min}$ value for the 49 ΔR_{np} is about 60. As a result, our normalized χ_n of 1.1 ± 0.1 is close to 1 within the error bar, which means that there are no significant unidentified systematic uncertainties. Therefore, similar to Ref. [42], the statistical error with a confidence level of 68.3% for the slope L is obtained using the $\chi^2_{\rm min}+1$ method.

Furthermore, we also constrain the slope L using the so-called model-independent ΔR_{np} of ^{48}Ca and ^{208}Pb determined by the CREX and PREX experiments [23, 33], as shown in Fig. 2. The obtained L of 45(32) MeV is very consistent with the result of 50(6) MeV determined by the compiled model-dependent ΔR_{np} of ^{48}Ca, ^{64}Ni, ^{124}Sn, and

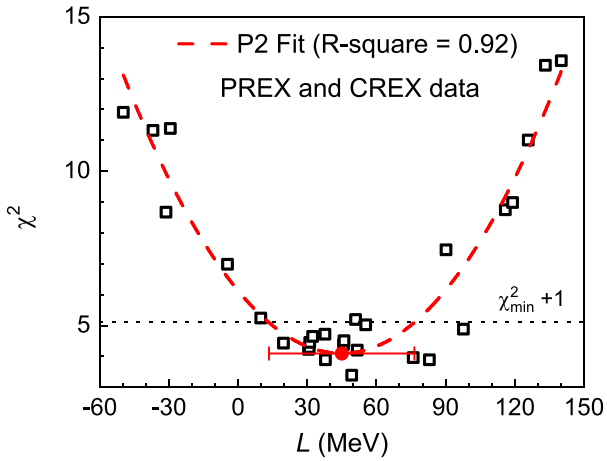

Fig. 2. (color online) Same as Fig. 1, but χ^2 are obtained by the two model-independent ΔR_{np} from the CREX and PREX experiments [23, 33].

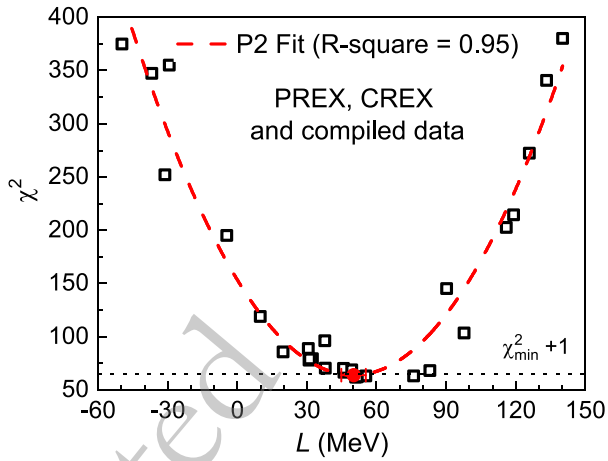

Fig. 3. (color online) Same as Fig. 1, but χ^2 are determined by all data used in Fig. 1 and Fig. 2.

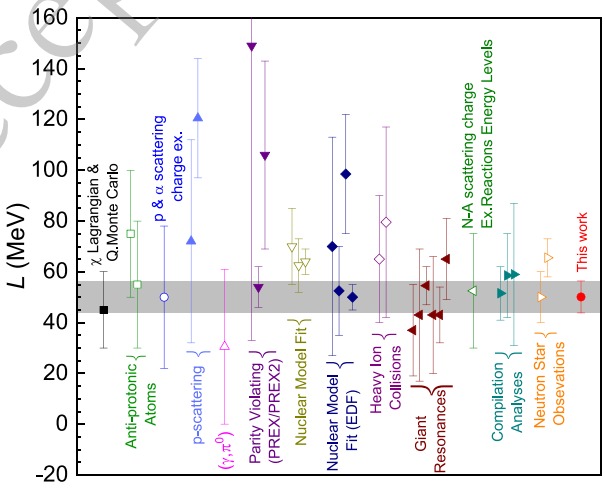

Fig. 4. (color online) Comparison of the obtained L in this work with the reported results from various methods, which were taken from Ref. [14]. Gray area indicates the uncertainty of our L.

^{208}Pb [27]. The difference of their centre values is only about 5 MeV, which would show the consistency of ΔR_{np} from different experiments.

Finally, see Fig. 3, the slope L is constrained to be 50(6) MeV using all fifty-one ΔR_{np} values, including the model-dependent and -independent data used in Fig. 1 and Fig. 2. Figure 4 shows a comparison of the obtained L in this work with the reported data from different observables and methodologies, see review article [14] and references cited therein for more details. Our L result constrained by the abundant ΔR_{np} data from various experiments has a high precision. Especially, our L value is consistent with the so-called world-averaged result, namely, a weighted mean value of 57.2(22) MeV obtained by these literature data in Fig. 4. Their difference is only about 7.2(64) MeV.

III. NEUTRON STAR RADIUS AND DISCUSSION

We further revisit the effects of our L on the neutron star radii $R_{1.4}$ at 1.4 solar-mass ($1.4\,M_\odot$). To easily understand the effects of the EoS parameters, the neutron star radii R can be empirically expressed as [4]

$$R^4 \propto \frac{\rho^2}{3\rho_0}\left[\frac{K_0}{3}\left(\frac{\rho}{\rho_0}-1\right)+\frac{Q_0}{18}\left(\frac{\rho}{\rho_0}-1\right)^2+L\delta^2\right], \qquad (2)$$

where $\delta=(\rho_n-\rho_p)/\rho$ stands for the asymmetry parameter, with ρ_n and ρ_p the neutron and proton densities, respectively. The $R_{1.4}$-L correlation deduced from various EoS parameter sets is relatively weak [4], and there is a model-dependent $R_{1.4}$ spread of around 2 km at one given L [4, 15]. Consequently, as indicated by Eq. 2, the L value alone is insufficient to characterize the $R_{1.4}$.

However, the effects of L on $R_{1.4}$ can be evaluated by adjusting the coupling constants associated with the vector-isovector meson ρ in relativistic mean-field Lagrangian, while the coupling strengths of isoscalar mesons are kept, more details see Ref. [5]. For instance, the linear $R_{1.4}$-L relationships were established by using such kinds of methods based on the TM1 and IUFSU EoS families [5], respectively. Similarly, we also deduce the $R_{1.4}$-L relationships from the DD-ME2 and TW99 EoS families, respectively. The matter in the core of neutron star is composed of neutrons, protons, electrons, and muons, and is assumed to be in β-equilibrium. For the core, we describe the EoS of uniform neutron star matter using the DD-ME2 and TW99 models. For the inner and outer crust regions, the EoS of nonuniform matters are generate by the Thomas-Fermi approximation and the Baym-Pethick-Sutherland, respectively. By fitting the deduced $R_{1.4}$-L relationships, see Fig 5, linear functions of $R_{1.4}=12.12+0.0189L$ and $R_{1.4}=11.03+0.0211L$ are ob-

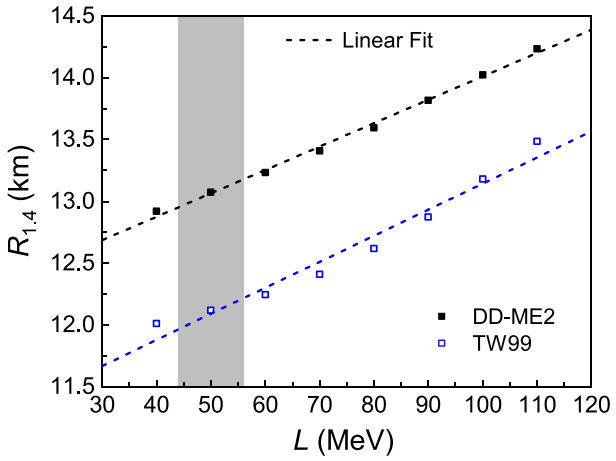

Fig. 5. (color online) The $R_{1.4}$-L correlations obtained by the DD-ME2 and TW99 EoS families. The dashed lines show the linear fit curves. The shaded area is the range of L constrained by this work.

tained for the DD-ME2 and TW99 families, respectively. These linear functions would be helpful to evaluate the effects of L on the $R_{1.4}$ determinations. The spread of 30-110 MeV for L would lead to a $R_{1.4}$ uncertainty of about 1.6 km for the same theoretical framework, see Fig. 5. It is comparable to the model-dependent $R_{1.4}$ uncertainty of about 2 km for the different EoS families [4, 15]. Compared to about 1.6 km $R_{1.4}$ uncertainty caused by the L spread of 30-110 MeV, the obtained L of 50(6) MeV in this work from finite nucleus system improves the $R_{1.4}$ precision (resulted only by L) by a factor of about 7 to be around 0.24 km at the same theoretical framework, see Fig. 5. Therefore, at the precision level of our L, the model-dependent $R_{1.4}$ uncertainty of about 2 km becomes more obvious [4, 15]. Furthermore, as shown in Fig. 5, there is also an obvious model-dependent $R_{1.4}$ difference of about 1 km between the DD-ME2 and TW99 EoS families. For the model-dependent $R_{1.4}$ difference between the TM1 and IUFSU EoS families, as shown in Fig. 15 in Ref. [5], which was explained by the difference of incompressibility coefficient K_0 [5], because the Q_0 value of −285 MeV for the TM1 is very close to the one of −290 MeV for the IUFSU EoS family [15]. Compared to the K_0 and L, the poorly known Q_0 has a large spread from ~ −1000 to ~ 1000 MeV [15]. We note that the DD-ME2 and TW99 families have almost the same K_0, but the Q_0 values are totally different, they are 478 MeV and −544 MeV, respectively [15]. Therefore, it is also interesting to further study the $R_{1.4}$ deviation caused by the poorly known Q_0 by using the DD-ME2 and TW99 EoS families. Anyway, the K_0 and Q_0 will largely influence the high-density behaviors of EoSs and the magnitude of $R_{1.4}$ of neutron stars.

IV. SUMMARY

The symmetry energy slope L at the saturation density was constrained by neutron skins from various experiments. The determined L of 50(6) MeV is consistent with the so-called world-averaged result from different observables and methodologies. Furthermore, based on the DD-ME2 and TW99 EoS families, the linear $R_{1.4}$-L relationships were established to study the effects of the newly constrained L on the radius determinations of 1.4 solar-mass neutron stars. Significant model-dependence of neutron star radius resulted by the different skewness parameter Q_0 was observed. Our L value effectively reduces the $R_{1.4}$ uncertainty of neutron star caused by the L spread with a factor of about 7 to be around 0.24 km at the same theoretical framework, which is smaller than the uncertainty of about 2 km from the different EoS families.

ACKNOWLEDGEMENTS

We would like to thank J. J. Li for the useful discussions and calculations.

References

[1] B. Li, L. Chen, and C. Ko, Phys. Rep. **464**, 113 (2008)
[2] J. M. Lattimer and M. Prakash, Science **304**, 536 (2004)
[3] J. M. Lattimer and M. Prakesh, Phys. Rep. **442**, 109 (2007)
[4] N. Alam, B. K. Agrawal, M. Fortin, H. Pais, C. Providência, A. R. Raduta, and A. Sulaksono, Phys. Rev. C **94**, 052801(R) (2016)
[5] J. Hu, S. Bao, Y. Zhang, K. Nakazato, K. Sumiyoshi, and H. Shen, Prog. Theor. Exp. Phys. **2020**, 043D01 (2020)
[6] B.-A. Li and M. Magno, Phys. Rev. C **102**, 045807 (2020)
[7] B.-A. Li, B.-J. Cai, W.-J. Xie, and N.-B. Zhang, Universe **7**, 182 (2021)
[8] J. Richter and B.-A. Li, Phys. Rev. C **108**, 055803 (2023)
[9] K. Huang, H. Shen, J. Hu, and Y. Zhang, Phys. Rev. C **109**, 045804 (2024)
[10] X. Viñas, P. Bano, Z. Naik, and T. R. Routray, Symmetry **16**, 215 (2024)
[11] U. Garg and G. Colò, Prog. Part. Nucl. Phys. **101**, 55 (2018)
[12] S. Shlomo, V. M. Kolomietz, and G. Colò, Eur. Phys. J. A **30**, 23 (2006)
[13] Z. Z. Li, Y. F. Niu, and G. Colò, Phys. Rev. Lett. **131**, 082501 (2023)
[14] H. Sotani, N. Nishimura, and T. Naito, Prog. Theor. Exp. Phys. **2022**, 041D01 (2022)
[15] B. Sun, S. Bhattiprolu, and J. M. Lattimer, Phys. Rev. C **109**, 055801 (2024)
[16] B. A. Brown, Phys. Rev. Lett. **85**, 5296 (2000)
[17] M. von Schmid, T. Aumann, S. Bagchi, S. Bönig, M. Csatlós, I. Dillmann, C. Dimopoulou, P. Egelhof, V. Eremin, T. Furuno *et al.*, Eur. Phys. J. A **59**, 83 (2023)
[18] J. T. Zhang, P. Ma, Y. Huang, X. L. Tu, P. Sarriguren, Z. P.

Li, Y. Kuang, W. Horiuchi, T. Inakura, L. Xayavong *et al*., Phys. Rev. C **108**, 014614 (2023)
[19] K. Yue, J. T. Zhang, X. L. Tu, C. J. Shao, H. X. Li, P. Ma, B. Mei, X. C. Chen, Y. Y. Yang, X. Q. Liu *et al*., Phys. Rev. C **100**, 054609 (2019)
[20] Y. Huang, S. Y. Xia, Y. F. Li, X. L. Tu, J. T. Zhang, C. J. Shao, K. Yue, P. Ma, Y. F. Niu, Z. P. Li *et al*., Phys. Lett. B **856**, 138902 (2024)
[21] Y. Huang, L. Xayavong, X. L. Tu, J. Geng, Z. P. Li, J. T. Zhang, and Z. H. Li, Phys. Lett. B **847**, 138293 (2023)
[22] A. Trzcińska, J. Jastrzebski, P. Lubiński, F. J. Hartmann, R. Schmidt, T. von Egidy, and B. Kłos, Phys. Rev. Lett. **87**, 082501 (2001)
[23] D. Adhikari, H. Albataineh, D. Androic, K. Aniol, D. S. Armstrong, T. Averett, C. Ayerbe Gayoso, S. Barcus, V. Bellini, R. S. Beminiwattha *et al*., Phys. Rev. Lett. **126**, 172502 (2021)
[24] G. A. Korolev, A. V. Dobrovolsky, A. G. Inglessi, G. D. Alkhazov, P. Egelhof, A. Estradé, I. Dillmann, F. Farinon, H. Geissel, S. Ilieva *et al*., Phys. Lett. B **780**, 200 (2018)
[25] M. Tanaka, M. Takechi, A. Homma, M. Fukuda, D. Nishimura, T. Suzuki, Y. Tanaka, T. Moriguchi, D. S. Ahn, A. Aimaganbetov *et al*., Phys. Rev. Lett. **124**, 102501 (2020)
[26] S. Terashima, H. Sakaguchi, H. Takeda, T. Ishikawa, M. Itoh, T. Kawabata, T. Murakami, M. Uchida, Y. Yasuda, M. Yosoi *et al*., Phys. Rev. C **77**, 024317 (2008)
[27] J. T. Zhang, X. L. Tu, P. Sarriguren, K. Yue, Q. Zeng, Z. Y. Sun, M. Wang, Y. H. Zhang, X. H. Zhou, and Y. A. Litvinov, Phys. Rev. C **104**, 034303 (2021)
[28] G. D. Alkhazov, M. N. Andronenko, A. V. Dobrovolsky, P. Egelhof, G. E. Gavrilov, H. Geissel, H. Irnich, A. V. Khanzadeev, G. A. Korolev, A. A. Lobodenko *et al*., Phys. Rev. Lett. **78**, 2313 (1997)
[29] I. Tanihata, H. Hamagaki, O. Hashimoto, Y. Shida, N. Yoshikawa, K. Sugimoto, O. Yamakawa, T. Kobayashi, and N. Takahashi, Phys. Rev. Lett. **55**, 2676 (1985)
[30] A. Krasznahorkay, M. Fujiwara, P. van Aarle, H. Akimune, I. Daito, H. Fujimura, Y. Fujita, M. N. Harakeh, T.Inomata, J. Jänecke *et al*., Phys. Rev. Lett. **82**, 3216 (1999)
[31] H. Sagawa, S. Yoshida, X.-R. Zhou, K. Yako, and H. Sakai, Phys. Rev. C **76**, 024301 (2007)
[32] J. Jastrzebski, A. Trzcińska, P. Lubiński, B. Kłos, F. J. Hartmann, T. von Egidy, and S. Wycech, Int. J. Mod. Phys. E **13**, 343 (2004)
[33] D. Adhikari, H. Albataineh, D. Androic, K. A. Aniol, D. S. Armstrong, T. Averett, C. Ayerbe Gayoso, S. K. Barcus, V. Bellini, R. S. Beminiwattha, *et al*., Phys. Rev. Lett. **129**, 042501 (2022)
[34] P.-G. Reinhard, X. Roca-Maza, and W. Nazarewicz, Phys. Rev. Lett. **129**, 232501 (2022)
[35] C. Mondal and F. Gulminelli, Phys. Rev. C **107**, 015801 (2023)
[36] T. Miyatsu, M.-K. Cheoun, K. Kim, and K. Saito, Phys. Lett. B **843**, 138013 (2023)
[37] T.-G. Yue, Z. Zhang, and L.-W. Chen, arXiv: 2406.03844v1 (2024).
[38] Z. Zhang and L.-W. Chen, Phys. Rev. C **108**, 024317 (2023)
[39] F. Sammarruca, Symmetry **16**, 34 (2024)
[40] J. M. Lattimer, Particles **6**, 30 (2023)
[41] B. T. Reed, F. J. Fattoyev, C. J. Horowitz, and J. Piekarewicz, Phys. Rev. Lett. **126**, 172503 (2021)
[42] Z. Zhang and L.-W. Chen, Phys. Lett. B **726**, 234 (2013)
[43] L.-W. Chen, C. M. Ko, B.-A. Li, and J. Xu, Phys. Rev. C **82**, 024321 (2010)
[44] X. Roca-Maza, M. Centelles, X. Viñas, and M. Warda, Phys. Rev. Lett. **106**, 252501 (2011)
[45] J. Friedrich and P.-G. Reinhard, Phys. Rev. C **33**, 335 (1986)
[46] M. Beiner, H. Flocard, N. Van Giai, and P. Quentin, Nucl. Phys. A **238**, 29 (1975)
[47] J. Dobaczewski, H. Flocard, and J. Treiner, Nucl. Phys. A **422**, 103 (1984)
[48] J. Gómez, C. Prieto, and J. Navarro, Nucl. Phys. A **549**, 125 (1992)
[49] F. Tondeur, M. Brack, M. Farine, and J. M. Pearson, Nucl. Phys. A **420**, 297 (1984)
[50] M. Rayet, M. Arnould, G. Paulus, and F. Tondeur, Astron. Astrophysics. **116**, 183 (1982)
[51] N. Van Giai and H. Sagawa, Phys. Lett. B **106**, 379 (1981)
[52] J. Bartel, P. Quentin, M. Brack, C. Guet, and H.-B. Håkansson, Nucl. Phys. A **386**, 79 (1982)
[53] E. Chabanat, P. Bonche, P. Haensel, J. Meyer, and R. Schaeffer, Nucl. Phys. A **635**, 231 (1998)
[54] H. Krivine, J. Treiner, and O. Bohigas, Nucl. Phys. A **336**, 155 (1980)
[55] G. A. Lalazissis, T. Nikšić, D. Vretenar, and P. Ring, Phys. Rev. C **71**, 024312 (2005)
[56] S. Typel and H. H. Wolter, Nucl. Phys. A **656**, 331 (1999)
[57] W. Long, H. Sagawa, J. Meng, and N. V. Giai, Europhys. Lett. **82**, 12001 (2008)
[58] W. Long, J. Meng, N. Van Giai, and S.-G. Zhou, Phys. Rev. C **69**, 034319 (2004)
[59] W.-H. Long, N. Van Giai, and J. Meng, Phys. Lett. B **640**, 150 (2006)
[60] G. A. Lalazissis, J. König, and P. Ring, Phys. Rev. C **55**, 540 (1997)
[61] M. Bender, K. Rutz, P.-G. Reinhard, J. A. Maruhn, and W. Greiner, Phys. Rev. C **60**, 034304 (1999)
[62] M. Rufa, P.-G. Reinhard, J. A. Maruhn, W. Greiner, and M. R. Strayer, Phys. Rev. C **38**, 390 (1988)
[63] P. Reinhard, M. Rufa, J. Maruhn, W. Greiner, and J. Friedrich, Z. Phys. A **323**, 13 (1986)